

Study of electric characteristics and diffusion effects of 2-methyl-9,10-di(2-naphthyl)anthracene doped with cesium fluoride by admittance spectroscopy

Ming-Ta Hsieh, Meng-Huan Ho, Kuan-Heng Lin, Jenn-Fang Chen, Teng-Ming Chen, and Chin H. Chen

Citation: *Applied Physics Letters* **96**, 133310 (2010); doi: 10.1063/1.3377921

View online: <http://dx.doi.org/10.1063/1.3377921>

View Table of Contents: <http://scitation.aip.org/content/aip/journal/apl/96/13?ver=pdfcov>

Published by the [AIP Publishing](#)

Articles you may be interested in

Phase transition characteristics under vacuum of 9,10-di(2-naphthyl)anthracene for organic light-emitting diodes

J. Vac. Sci. Technol. A **32**, 020601 (2014); 10.1116/1.4831935

Study of electrical characterization of 2-methyl-9, 10 - d i (2-naphthyl)anthracene doped with tungsten oxide as hole-transport layer

Appl. Phys. Lett. **95**, 033501 (2009); 10.1063/1.3173824

Studies of the degradation mechanism of organic light-emitting diodes based on tris (8-quinolinolate)aluminum Alq and 2-tert-butyl-9,10-di(2-naphthyl)anthracene TBADN

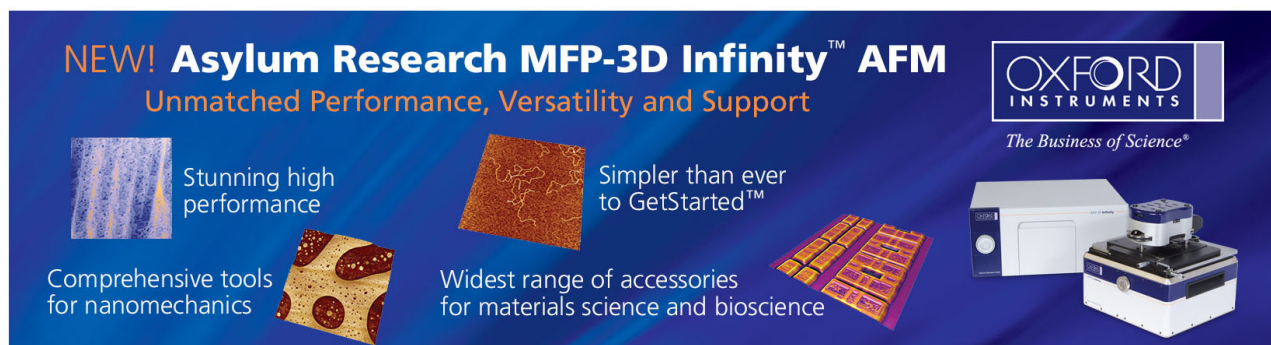
J. Appl. Phys. **105**, 034905 (2009); 10.1063/1.3072622

Study of efficient and stable organic light-emitting diodes with 2-methyl-9,10-di(2-naphthyl)anthracene as hole-transport material by admittance spectroscopy

Appl. Phys. Lett. **94**, 023306 (2009); 10.1063/1.3072616

Highly efficient deep blue organic electroluminescent device based on 1-methyl-9,10-di(1-naphthyl)anthracene

Appl. Phys. Lett. **89**, 252903 (2006); 10.1063/1.2409367



NEW! Asylum Research MFP-3D Infinity™ AFM
Unmatched Performance, Versatility and Support

OXFORD INSTRUMENTS
The Business of Science®

Stunning high performance
Simpler than ever to GetStarted™

Comprehensive tools for nanomechanics
Widest range of accessories for materials science and bioscience

Study of electric characteristics and diffusion effects of 2-methyl-9,10-di(2-naphthyl)anthracene doped with cesium fluoride by admittance spectroscopy

Ming-Ta Hsieh,^{1,a)} Meng-Huan Ho,^{2,a)} Kuan-Heng Lin,³ Jenn-Fang Chen,¹ Teng-Ming Chen,² and Chin H. Chen³

¹Department of Electrophysics, National Chiao Tung University, Hsinchu 300, Taiwan

²Department of Applied Chemistry, National Chiao Tung University, Hsinchu 300, Taiwan

³Display Institute, Microelectronics and Information Systems Research Center, National Chiao Tung University, Hsinchu 300, Taiwan

(Received 30 June 2009; accepted 11 March 2010; published online 1 April 2010)

In this work, the admittance spectroscopy studies show that doping cesium fluoride (CsF) into 2-methyl-9,10-di(2-naphthyl)anthracene (MADN) can greatly decrease the resistance of MADN and raises the Fermi level from deep level to only 0.1 eV below the lowest unoccupied molecular orbital, resulting in enhancing the electron injection. In addition, the diffusion width of CsF from doped MADN layer into tris(8-quinolinolato)aluminum is clearly observed by capacitance-frequency measurement and is about 9.4 nm. Moreover, the diffusion width is significant to be affected by external thermal. © 2010 American Institute of Physics. [doi:10.1063/1.3377921]

Organic light-emitting diode (OLED) has attached much attention due to their potential in flexible electronic paper, flat-panel displays, and lighting.^{1,2} However, the intrinsic properties of low power efficiency and high driving voltage limit their development. Recently, electrical doping is commonly adopted in the OLED due to that highly conductive *p*- and *n*-doped layers can be utilized to enhance the carrier injection and power efficiency.³⁻⁷ Accordingly, understanding the dynamics and the electrical characteristics of the electrical doping layers is critically important for adopting electrical doping techniques in the OLED. In a multilayer OLED, each layer can be treated as a resistance-capacitance (*RC*) unit and also shows an independent *RC* property, and thus the geometric and electrical characteristics can be investigated separately by admittance spectroscopy (AS). As a result, the electrical characteristics of each layer can be determined by AS with a suitable equivalent circuit model.^{8,9}

2-methyl-9,10-di(2-naphthyl)anthracene (MADN) has been shown to be an efficient blue host material.¹⁰ Moreover, MADN was discovered to exhibit an ambipolar transporting property¹¹ and can be used as host material for *p*-type dopant tungsten oxide.¹² In this paper, we further report the development of the *n*-doped transport layer using the ambipolar MADN as a host, in which cesium fluoride (CsF) is served as *n*-dopant. The AS studies show that the incorporation of CsF into MADN can greatly reduce the resistance and activation energy of MADN layer resulting in improving electron injection, which in turn demonstrates that MADN doped with CsF could also be an efficient *n*-doped transport layer. In addition, the diffusion effect of CsF between MADN and tris(8-quinolinolato)aluminum (Alq₃) was also investigated using capacitance-frequency (*C-F*) measurement.

A series of electron-only devices were fabricated for studying the effect of CsF incorporation into MADN. The structures of devices A, B, C, and D were indium-tin-oxide (ITO)/Alq₃ (30 nm)/aluminum (Al) (150 nm), ITO/MADN

(30 nm)/Al (150 nm), ITO/Alq₃ (30 nm)/MADN (30 nm)/Al (150 nm), and ITO/Alq₃ (30 nm)/MADN: 30% CsF (30 nm)/Al (150 nm), respectively.

Figure 1 shows the 300 K *C-F* spectra measured at zero bias on the studied devices. All spectra show a capacitance drop at an inflexion frequency around 0.1 MHz, suggesting the presence of a geometric *RC* time constant effect of series resistance due to lead/contact resistance.¹³ In devices A and B, the capacitances before drops are the constants of 10.5 and 9.1 nF whose values are comparable to the values of 10.6 and 9.03 nF, determined from a parallel-capacitor model with $\epsilon_r=4$ and 3.4 for Alq₃ and MADN, respectively.¹⁴ Moreover, the value of capacitance (4.9 nF) in device C shows an excellent agreement with the series combination of devices A and B. As a result, the equivalent circuit models for devices A, B, and C are developed and are shown in the inset of Fig. 1, where C_{A1} , R_{A1} and C_{M1} , R_{M1} represent the geometric capacitance and resistance of the Alq₃ layer (AL) and the MADN layer, respectively, and R_s represents the series resistance. In these models, however, R_{A1} and R_{M1} can be treated as an open circuit even at 420 K due to the intrinsic

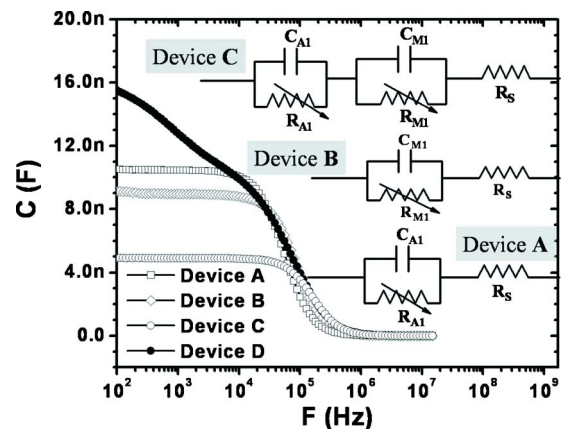


FIG. 1. (Color online) Spectra of the *C-F* at 300 K, measured on devices A, B, C, and D. The equivalent circuit models for devices A, B, and C are shown in the inset.

^{a)}Authors to whom correspondence should be addressed. Electronic addresses: mthsieh.ep94g@nctu.edu.tw and kinneas.ac94g@nctu.edu.tw.

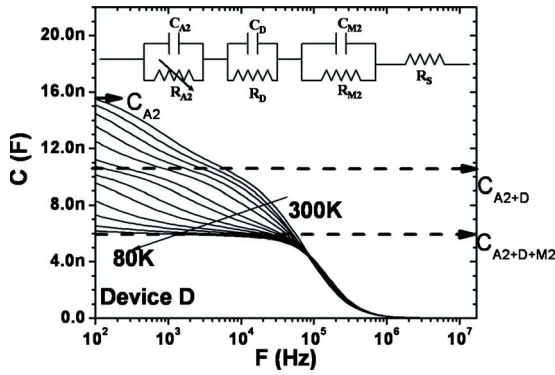


FIG. 2. (Color online) Temperature-dependent C - F spectra measured from 300 to 80 K for device D. The equivalent circuit model for device D is shown in the inset.

sic high resistivity property. Therefore, the limited electrical characteristics of these devices can be obtained by AS measurements. In device D, the MADN doped with CsF layer (MDL) is expected to show a low resistivity property due to the high CsF incorporation so that R_{M1} can be treated as a short circuit and only C_{A1} can be observed at low frequency region. However, the capacitance of device D at 100 Hz is 15.5 nF whose value is larger than that of C_{A1} . Moreover, as frequency increases, the capacitance drops and reaches a plateau whose value equals to C_{A1} approximately. Accordingly, the geometric RC time constant drop between 15.5 and 10.5 nF is suggested to be contributed by the AL with partial CsF diffused from the MDL resulting in decreasing the resistivity of the partial AL. As a result, an equivalent circuit model for device D is developed and is shown in the inset of Fig. 2, where C_{A2} , R_{A2} ; C_D , R_D ; and C_{M2} , R_{M2} represent the geometric capacitance and resistance of the Alq_3 without CsF diffusion layer (AWCL), the Alq_3 diffused with CsF layer (ADL), and the MDL, respectively. In this model, three geometric RC time constant drops for the ADL, MDL, and series resistance can be observed in the C - F measurement. However, the spectrum of device D in Fig. 1 shows only two capacitance drops, which is due to that the resistance of the MDL is too small to resolve from the series resistance at 300 K. In Fig. 1, the capacitance of device D at 100 Hz can clearly determine the thickness of the AWCL which in turn indicates that the diffusion width of CsF in the AL is about 9.4 nm.

Figure 2 shows temperature-dependence C - F spectra of device D that was measured from 300 to 80 K for avoiding an external thermal effect. As shown, two significant temperature-dependence capacitance drops and one temperature-independence capacitance drop were observed. Between 15.5 nF and ~ 10.6 nF, the inflexion frequency is associated with the inverse RC time constant of the ADL. As temperature decreases, another capacitance drop is resolved from series resistance and drops between ~ 10.6 and 6 nF, in which the inflexion frequency is associated with the RC time constant of the MDL. Note that the inflexion frequencies of ADL and MDL in the C - F spectra can be more clearly seen in the conductance (G)/ F - F peaks of Figs. 4(a) and 4(b), respectively. According to the temperature-dependent peaks, the activation energies (E_a) of both layers can be obtained by the relationship of $F = F_0 \exp(-E_a/KT)$ (where F is G/F peak frequency, F_0 is pre-exponential factor, K is Boltzmann's constant, and T is the temperature) and are shown in plots of $\ln(F)$ versus $1000/T$ in Fig. 5. As shown, the E_a of

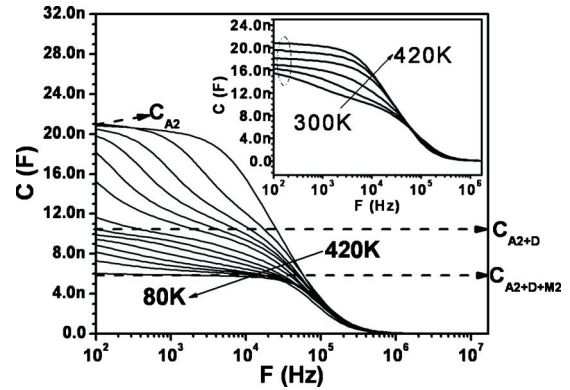


FIG. 3. (Color online) Temperature-dependent C - F spectra measured from 420 to 80 K for device D. The C - F spectra measured from 300 to 420 K is shown in the inset.

the ADL and the MDL before high temperature measurement were 0.219 eV and 0.1 eV, respectively. In addition, the capacitance at 100 Hz and 80 K is about 6 nF whose value is larger than 4.9 nF obtained from device C. This can be explained by a change in the permittivity of MADN due to the heavy CsF incorporation.

The inset of Fig. 3 plots the C - F spectra of device D measured from 300 to 420 K for studying the thermal effect on CsF diffusion. As shown, the capacitance at 100 Hz is observably increased from 15.5 to 21 nF indicating that the diffusion width of CsF in AL is increased from 9.6 to 14.8 nm. Furthermore, as temperature decreases from 420 to 80 K, the inflexion frequencies of the ADL and the MDL also can be observed clearly in Fig. 3. In Figs. 4(c) and 4(d), the temperature-dependent peaks are assigned to be associated with the RC time constants of the ADL and the MDL after 420 K measurement, respectively. Moreover, the E_a of the ADL and the MDL after 420 K measurement were shown in Fig. 5. As shown, the E_a of the ADL and the MDL after 420 K measurement were both increased from 0.219 eV and 0.1 eV to 0.509 eV and 0.219 eV, respectively. Owing to that the E_a represents the energy separation between the edge of the lowest unoccupied molecular orbital (LUMO) and Fermi level, the increase in E_a in the MDL indicates that the external thermal decreases the electron concentration in the MDL due to that the partial CsF were further diffused into Alq_3

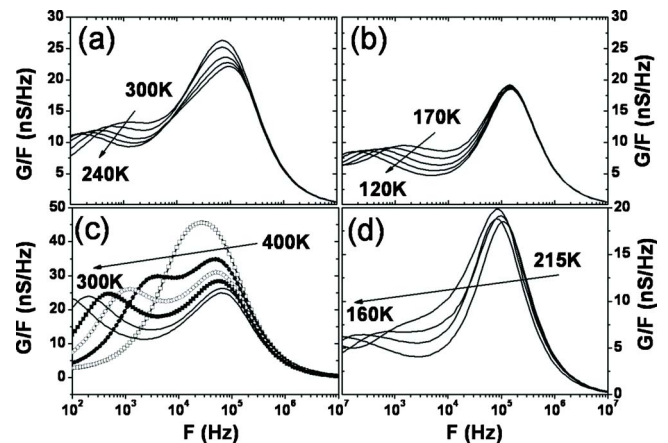


FIG. 4. (Color online) Temperature-dependent G/F - F spectra at zero bias for device D. (a) and (b) measured before high temperature measurement. (c) and (d) measured after 420 K measurement.

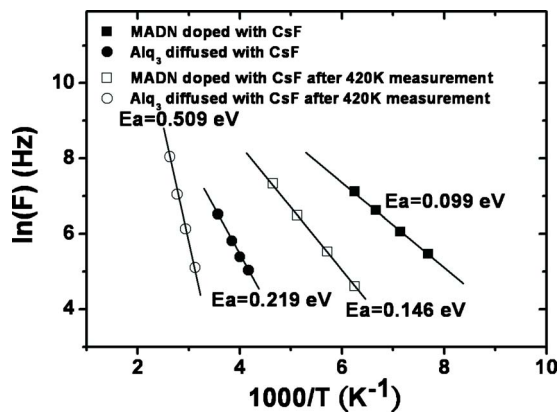


FIG. 5. (Color online) Plots of $\ln(F)$ vs $1000/T$. The F is derived from the temperature-dependent peaks in the G/F - F spectra in Fig. 4.

layer by the increase in temperature resulting in increasing this separation. In the ADL, although the amount of CsF is increased after 420 K measurement but the effective thickness of the ADL is increased simultaneously. Therefore, the overall electron concentration in the ADL after 420 K measurement is decreased resulting in the increase in E_a .

Furthermore, we also fabricated an OLED device with structure of ITO/ CF_x/N , N' -bis-(1-naphthyl)- N,N' -diphenyl,1,1'-biphenyl-4,4'-diamine (60 nm)/Alq₃ (65 nm)/MADN: 30% CsF (10 nm)/Al to demonstrate the efficacy of the layer of MADN doped with CsF. The device can achieve the efficiency of 2.0 lm/W at 5.2 V and 20 mA/cm². The drive voltage of this device is much lower than that of the device with conventional LiF/Al cathode (6.3 V and 1.8 lm/W), the detailed device performance will be reported elsewhere.¹⁵ Significantly, inducing the layer of MADN doped with CsF can reduce the drive voltage, which agrees completely the results of AS measurement and suggests that the n -doped layer of MADN doped with CsF could be applied in OLED devices.

In summary, the details of electrical characteristics of the MADN doped with CsF were investigated by employing temperature-dependence AS with the equivalent circuit model. The incorporation of CsF into MADN can greatly

decrease the resistance of MADN and raises the Fermi level from deep level to only 0.1 eV below LUMO band resulting in decreasing the width of the electron injection barrier between MADN and Al. As a result, the electron injection from cathode can be enhanced when the MADN doped with CsF is adopted as an n -doped electron transport layer. In addition, the diffusion width of CsF from the MDL into the AL is observed to about 9.4 nm by C - F measurement and is significant to be affected by external thermal. This information is very useful for design consideration when MDL is adopted as the hole transport layer in the OLED.

The authors would like to thank the National Science Council of the Republic of China, Taiwan for financially supporting under Contract Nos. NSC 97-2112-M-009-014MY3 and NSC 97-2218-E-009-003.

- ¹M. K. Mathai, V. E. Choong, S. A. Choulis, B. C. Krummacker, and F. So, *Appl. Phys. Lett.* **88**, 243512 (2006).
- ²T. B. Singh and N. S. Sariciftci, *Annu. Rev. Mater. Res.* **36**, 199 (2006).
- ³J. H. Lee, M. H. Wu, C. C. Chao, H. L. Chen, and M. K. Leung, *Chem. Phys. Lett.* **416**, 234 (2005).
- ⁴S. H. Kim, J. Jang, and J. Y. Lee, *Appl. Phys. Lett.* **91**, 103501 (2007).
- ⁵J. Blochwitz, M. Pfeiffer, T. Fritz, and K. Leo, *Appl. Phys. Lett.* **73**, 729 (1998).
- ⁶J. Huang, M. Pfeiffer, A. Werner, J. Blochwitz, S. Liu, and K. Leo, *Appl. Phys. Lett.* **80**, 139 (2002).
- ⁷C. Ganzorig and M. Fujihira, *Appl. Phys. Lett.* **77**, 4211 (2000).
- ⁸M. T. Hsieh, C. C. Chang, J. F. Chen, and C. H. Chen, *Appl. Phys. Lett.* **89**, 103510 (2006).
- ⁹M. H. Ho, M. T. Hsieh, T. M. Chen, J. F. Chen, S. W. Hwang, and C. H. Chen, *Appl. Phys. Lett.* **93**, 083505 (2008).
- ¹⁰M. T. Lee, H. H. Chen, C. H. Tsai, C. H. Liao, and C. H. Chen, *Appl. Phys. Lett.* **85**, 3301 (2004).
- ¹¹M. H. Ho, Y. S. Wu, S. W. Wen, M. T. Lee, T. M. Chen, C. H. Chen, K. C. Kwok, S. K. So, K. T. Yeung, Y. K. Cheng, and Z. Q. Gao, *Appl. Phys. Lett.* **89**, 252903 (2006).
- ¹²M. H. Ho, M. T. Hsieh, K. H. Lin, T. M. Chen, J. F. Chen, and C. H. Chen, *Appl. Phys. Lett.* **94**, 023306 (2009).
- ¹³W. Brütting, H. Riel, T. Beierlein, and W. Riess, *J. Appl. Phys.* **89**, 1704 (2001).
- ¹⁴S. Berleb and W. Brütting, *Phys. Rev. Lett.* **89**, 286601 (2002).
- ¹⁵M. H. Ho, M. Y. Liu, K. H. Lin, C. H. Chen, and C. W. Ching, "Efficient single-layer small molecule blue OLEDs based on a multifunctional bipolar transport material," SID Int. Symp. Digest Tech. Papers (to be published).